Water Research 145 (2018) 220–230

Contents lists available at ScienceDirect

Water Research

journal homepage: www.elsevier.com/locate/watres

Active chlorine mediated ammonia oxidation revisited: Reaction mechanism, kinetic modelling and implications

Changyong Zhang [a, 1], Di He [b, 1], Jinxing Ma [a], T. David Waite [a, *]

[a] School of Civil and Environmental Engineering, University of New South Wales, Sydney, NSW, 2052, Australia
[b] Guangzhou Key Laboratory of Environmental Catalysis and Pollution Control, School of Environmental Science and Engineering, Institute of Environmental Health and Pollution Control, Guangdong University of Technology, Guangzhou, 510006, China

ARTICLE INFO

Article history:
Received 13 June 2018
Received in revised form
29 July 2018
Accepted 10 August 2018
Available online 11 August 2018

Keywords:
Electrochemical advanced oxidation process
Ammonia oxidation
Active chlorine
Kinetic model

ABSTRACT

Ammonia nitrogen removal from wastewaters has gained much attention in recent decades as a result of the environmental problems associated with discharge of excessive amounts of this critical nutrient including eutrophication of receiving waters, generation of offensive odours as a result of organism decay and complications associated with the disinfection of water supplies. While removal via biological processes represents the principal means by which a reduction in dissolved nitrogen concentrations is achieved, an electrochemical advanced oxidation process has been proposed as a potentially effective alternate means of removing ammonia from wastewaters with the removal associated with the *in situ* generation of oxidants (particularly active chlorine) at the anode. Here we describe the influence of key factors on the rate and extent of ammonia nitrogen removal in an electrochemical cell with a Ti/IrO_2-RuO_2 anode and Ti cathode. The rate of ammonia removal was found to be dependent on both current density and initial chloride concentration with ~95% ammonia removed from a 20 mM Cl^- solution within approximately 40 min at a current density of 3 mA cm^{-2}, resulting in an energy consumption of 126 kWh kg^{-1} NH_4^+-N. Additionally, we show that by-products formation is effectively suppressed during the electrolysis process. A mechanistically-based kinetic model incorporating the key processes operating in the ammonia electro-oxidation process was developed with particular attention given to (i) anodic generation of active chlorine and other chloride-related by-products, (ii) active chlorine mediated ammonia oxidation. The results demonstrate that the electrochemical advanced oxidation process is a promising technology for treatment of ammonia-containing wastewaters with advantages including simplicity, safety and effectiveness.

1. Introduction

Ammonia removal from wastewaters has attracted much attention in recent decades given the concerns associated with discharge of this critical nutrient with particular problems including eutrophication of receiving waters, the generation of offensive odours and complications associated with the disinfection of water supplies (Buffle et al., 2004; Huang et al., 2008). A variety of ammonia removal technologies including air stripping (Bonmatı and Flotats, 2003), ion exchange (Jorgensen and Weatherley, 2003), adsorption (Wang et al., 2006), chemical precipitation (Li et al., 1999), electrochemical stripping (Tarpeh et al., 2018; Zhang et al., 2017), biological nitrification/denitrification (Kalyuzhnyi et al., 2006) and break-point chlorination (Pressley et al., 1972) have been applied extensively in the treatment of municipal and industrial wastewaters with each of these technologies exhibiting particular limitations. For example, air stripping consumes large amounts of energy and may result in air pollution problems when ammonia is transformed from aqueous to gas phase. Additionally, this technology exhibits poor removal efficiency at low ammonia concentrations (Obaid-ur-Rehman and Beg, 1990). Biological methods require a series of reactors to achieve the range of functions required (*i.e.*, nitrification, denitrification and solid-liquid separation) with the denitrification efficiency largely constrained by the biodegradable organic content in the wastewater (Ruiz et al., 2003). Breakpoint chlorination possesses risks related to the transport, storage and the handling of active

* Corresponding author.
E-mail addresses: changyong.zhang@unsw.edu.au (C. Zhang), di.he@gdut.edu.cn (D. He), jinxing.ma@unsw.edu.au (J. Ma), d.waite@unsw.edu.au (T.D. Waite).
[1] These authors contribute equally to this work.

https://doi.org/10.1016/j.watres.2018.08.025
0043-1354/

chlorine with challenges also associated with the optimization of the dosing of active chlorine.

In recent years, an electrochemical advanced oxidation process (EAOP) has emerged as a promising approach to ammonia removal with advantages including minimal production of secondary waste, amenability to automation, versatility, and safety (Li and Liu, 2009; Pérez et al., 2012a). It has been reported that EAOPs are effective for the treatment of ammonia-containing wastewaters from tanneries (Vlyssides and Israilides, 1997), power plants (Vanlangendonck et al., 2005), municipal sources (Li and Liu, 2009) and landfills (Ye et al., 2016).

Ammonia (in either ammonium ion (NH_4^+) or deprotonated $NH_{3(aq)}$ forms) can be removed by (i) direct anodic oxidation and/or (ii) indirect oxidation mediated by the electro-generated active chlorine. In the direct oxidation pathway, NH_3 is firstly adsorbed to the anode surface and subsequently decomposed, principally to harmless nitrogen gas, as a result of anodic electron transfer as shown in Eq. (1) (Kapałka et al., 2010; Kim et al., 2006; Zöllig et al., 2015b):

$$2NH_3 + 6OH^- \rightarrow N_2 + 6H_2O + 6e^- \quad (1)$$

However, direct ammonia oxidation requires the adjustment of wastewater pH to values greater than the pK_a of the NH_4^+/NH_3 acid-base pair (i.e., pH > 9.25) because NH_4^+ cannot be oxidized directly at the anode (Zöllig et al., 2015a). Furthermore, the low reaction rate and high cost of the electrodes (usually platinum) restricts the practical application of this technology (Zöllig et al., 2015b).

Indirect oxidation, which takes advantage of *in situ* generation of active chlorine at the anode to oxidize ammonia to nitrogen gas, is more commonly used (Ji et al., 2017; Kapałka et al., 2010; Li and Liu, 2009; Zhang et al., 2018b). This approach is much faster, more efficient and cost effective than direct oxidation provided sufficient chloride ion (>300 mg L^{-1}) is present in the wastewater stream (Kim et al., 2006). The overall reactions resulting in N_2 production are as follows:

$$2Cl^- \rightarrow Cl_2 + 2e^- \quad (2)$$

$$Cl_2 + H_2O \rightarrow HOCl + H^+ + Cl^- \quad (3)$$

$$2NH_4^+ + 3HOCl \rightarrow N_2 + 3H_2O + 5H^+ + 3Cl^- \quad (4)$$

Limited insight regarding the precise mechanism and reaction kinetics of the active chlorine-mediated ammonia oxidation process is currently available. Traditionally, it has been considered that the indirect electrochemical ammonia oxidation process (EAOP) occurs via a mechanism similar to that of the intensively studied breakpoint chlorination. That is, ammonia first reacts with the active chlorine species (HOCl or OCl^-) and, stepwise, generates chloramine species, i.e., monochloramine, dichloramine and trichloramine, and finally nitrogen gas when the active chlorine/ammonia mole ratio gradually reaches 1.5 (Mergerum et al., 1978; Qiang and Adams, 2004). However, results of a number of electrochemical indirect ammonia oxidation studies indicate that the transformation of ammonia into nitrogen gas takes place at the very beginning of the electrolysis process and long before an active chlorine/ammonia mole ratio of 1.5 is attained (Kim et al., 2006; Li and Liu, 2009; Vanlangendonck et al., 2005). These findings suggest that the mechanism of EAOP differs from that of the conventional breakpoint chlorination process and, as such, requires clarification. Not surprisingly, given the variety of Faradaic reactions that may occur at both anode and cathode as well as the various solution phase reactions that may influence the rate and extent of ammonia oxidation, there has been limited attempt to develop mechanistically-based models of the overall process. As such, the objectives of this work are to (i) determine the effects of operating parameters such as initial chloride concentration and current density on the rate and extent of ammonia removal, and (ii) development of a detailed mechanistically-based kinetic model providing insight into the complex interactions that occur during electrochemically-mediated ammonia oxidation processes that will assist in optimising implementation of the technology.

2. Materials and methods

2.1. Chemical reagents

All solutions were prepared using ultrapure 18 MΩ cm Milli-Q water (MQ, Millipore). Analytical grade chemicals, *i.e.*, ammonium sulfate, sodium sulfate, sodium chlorate, sodium perchlorate, sodium hypochlorite, etc., were purchased from Sigma-Aldrich (or as otherwise stated) and used without further refinement.

2.2. Experimental setup

The batch mode experiments were conducted in an open Plexiglass cubic cell at room temperature (25 °C). The commercial Ti/IrO_2-RuO_2 electrode purchased from BaoJi Changli Special Metal Co., Ltd served as the anode with a size of 10 × 10 cm^2 and a thickness of 0.1 cm. A piece of titanium plate was used as the cathode (BaoJi Changli Special Metal Co., Ltd) with the same dimensions as the anode. Both the anode and cathode were placed vertically and parallel to each other with the gap between the two electrodes maintained at 8 cm (Fig. S1).

2.3. Experimental methods and calculations

A range of factors influencing ammonia removal in the electrochemical advanced oxidation process was investigated including applied current density, initial Cl^- concentration, initial pH (pH_0) and initial ammonia concentration. During our experiments, a DC power source was used to provide constant current densities (ranged from 1 to 5 mA cm^{-2}) for the electrochemical cell. Initial Cl^- concentrations varied from 5 mM to 50 mM. Wastewater pH_0 values were adjusted using either 1 M NaOH or 1 M H_2SO_4. Each experiment was operated in batch mode and lasted for 90 min. Samples were taken from the electrochemical cell every 5 min for analysis of ammonium, nitrite, nitrate, chloride, chlorate and perchlorate concentrations using an ICS-3000 ion chromatograph (Dionex, U.S.). The DPD method was used to determine the concentrations of active chlorine and chloramine that were generated during electrolysis (APHA, 2012).

Current efficiency and energy consumption are two key parameters that may be used to evaluate the performance of an electrochemical technology (Ma et al., 2018; Zhang et al., 2018a). Current efficiency can be expressed as:

$$CE = \frac{n_i \times F \times (C_0 - C_t) \times V}{M \times \int_0^t IAdt} \times 100 \quad (5)$$

where C_0 is the initial concentration (mg L^{-1}) of NH_4^+-N, C_t is the concentration (mg L^{-1}) of NH_4^+-N at electrolysis time t (s), V represents the volume of the electrolyte (0.09 L), M is the molar mass of NH_4^+-N (14 g mol^{-1}), I is the current density (A m^{-2}), A is the effective surface area of the electrodes (0.01 m^2), F represents the Faraday constant (96485.3 C mol^{-1}) and n represents the number of electrons needed for the oxidation of 1 mol of NH_4^+-N (3 for oxidation of NH_4^+-N to N_2). The prediction of required ammonia

degradation time was obtained based on kinetic modelling data of time when NH_4^+-N concentration decreased below 1 mg L^{-1}.

Specific energy consumption (kWh kg^{-1} N) can be calculated as shown in Eq. (6):

$$EC = \frac{\int_0^t UIAdt}{3.6 \times (C_0 - C_t) \times V} \quad (6)$$

where U is the voltage of the electrochemical cell (V).

2.4. Kinetics modelling

According to a hypothesized reaction set describing all key chemical reactions occurring in the system, the concentrations of reactants and products (given specific initial conditions and rate constants) predicted to be present at any given time during the electrochemically-mediated active chlorine production and ammonia oxidation processes were determined by numerically solving the differential equations corresponding to the rate expressions for the hypothesized reactions using the kinetic modelling software Kintek Explorer (https://kintekcorp.com/) (Johnson et al., 2009, Qiu et al., 2015). Sensitivity analysis was undertaken using the kinetic modeling software Kintecus (http://kintecus.com/) by determining eigenvectors following previously published methods (Pham and Waite, 2008; Vajda et al., 1985; Xing et al., 2018).

3. Results

3.1. Chlorine evolution

The electrochemical system was first employed for examination of the evolution of chlorine species in the absence of ammonia at initial Cl^- concentrations of 10 mM and 20 mM under three different current densities (*i.e.*, 1, 3 and 5 mA cm^{-1}). As illustrated in Fig. 1, the gradual loss of Cl^- with a concomitant increase in active chlorine concentration indicated that Cl^- was converted into active chlorine at the anode surface (Reactions 1–6 in Table 1). Higher current density and initial Cl^- concentration resulted in faster active chlorine formation and higher steady state concentrations of active chlorine. For example, when an initial Cl^- concentration of 20 mM was applied during the electrolysis, steady-state active chlorine concentrations of 1.4–1.5, 2.7–2.9 and 3.3–3.5 mM were obtained at current densities of 1, 3 and 5 mA cm^{-1} respectively. A similar dependence was observed for the 10 mM Cl^- case with active chlorine concentrations reaching 0.8–0.9, 1.3–1.5 and 1.5–1.8 mM at current densities of 1, 3 and 5 mA cm^{-1} respectively.

3.2. Active chlorine-mediated ammonia oxidation

Fig. 2 demonstrates the effects of current density and Cl^- concentration on the removal of ammonia during 90-min reaction. It can be seen from these results that a higher current density leads to more rapid ammonia oxidation. When a current density of 1 mA cm^{-2} was applied, only 9.0% of NH_4^+-N could be degraded in 40 min at an initial Cl^- concentration of 10 mM. The removal rates increased dramatically to 43.2% and 88.0% on increasing the current density to 3 and 5 mA cm^{-2} respectively. A similar trend was observed for the 20 mM Cl^- case while enhanced ammonia removal rates (*i.e.*, 17.8%, 87.5%, and 97.7%) were observed following 90-min operation at current densities of 1–5 mA cm^{-2}.

The variation of NH_4^+-N concentrations for different initial Cl^- concentrations is presented in Fig. S2. An initial Cl^- concentration of 5 mM was too low to achieve an effective result. When the Cl^- concentration was higher than 10 mM, the treatment was

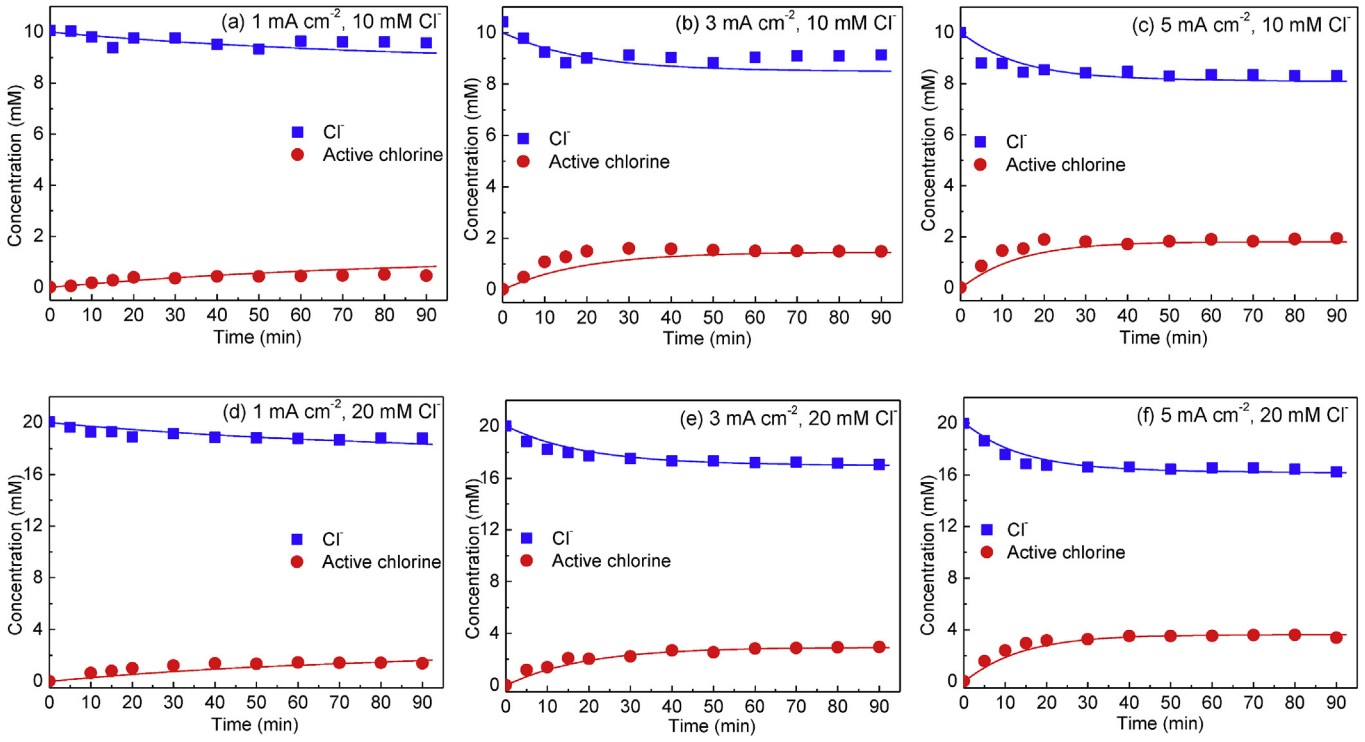

Fig. 1. Variation of Cl^- and active chlorine concentrations during the electrolysis of solutions containing different initial concentrations of Cl^- at current densities of 1–5 mA cm^{-1} and initial pH of 6. (a) I = 1 mA cm^{-1} and $[Cl^-]_0$ = 10 mM, (b) I = 3 mA cm^{-1} and $[Cl^-]_0$ = 10 mM, (c) I = 5 mA cm^{-1} and $[Cl^-]_0$ = 10 mM, (d) I = 1 mA cm^{-1} and $[Cl^-]_0$ = 20 mM, (e) I = 3 mA cm^{-1} and $[Cl^-]_0$ = 20 mM and (f) I = 5 mA cm^{-1} and $[Cl^-]_0$ = 10 mM. Solid lines represent the results of kinetic modelling.

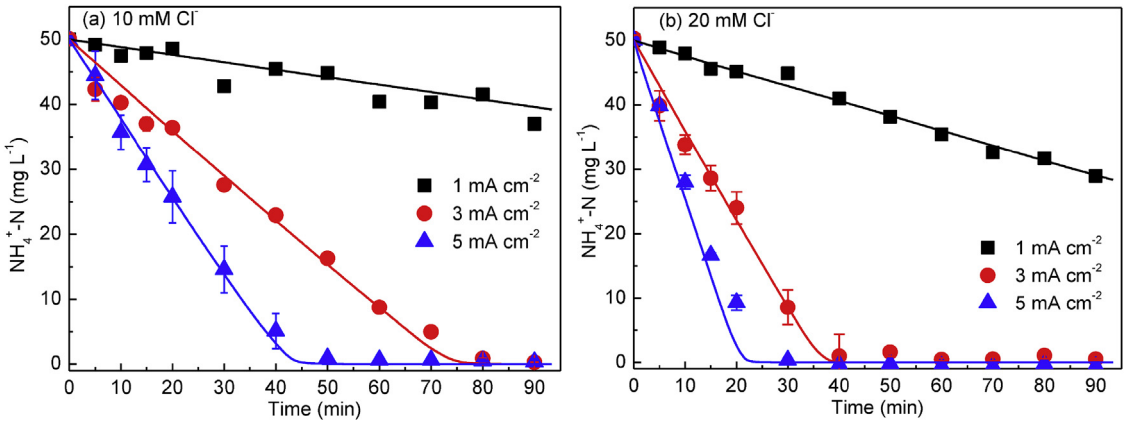

Fig. 2. NH_4^+-N removal at different current densities with initial Cl^- concentrations of (a) 10 mM and (b) 20 mM. Initial pH 6.0. Solid lines represent the results of kinetic modelling.

satisfactory, with the near-complete ammonia removal in 10, 40 and 80 min in the solutions containing 50, 20 and 10 mM Cl^-, respectively.

Initial pH was observed to exert much less significant influence on ammonia removal than either current density or Cl^- concentration in our electrochemical system. As can be seen from Fig. S3, the degradation of ammonia exhibited little difference for various initial pH conditions ($pH_0 = 3$, 6 and 9). Bulk solution pH decreased during the electrolysis process to similar values whatever the initial pH (Fig. S4) with this decrease a result of the abundant generation of H^+ through both hypochlorite generation and indirect ammonia oxidation reactions (reactions 3 and 4) and as a result of other side-reactions such as water splitting (Fig. S4). In addition, the insignificant effect of initial pH on ammonia removal could be attributed to the fact that ammonia degradation mainly takes place close to the anode surface where the local pH is likely to be minimally affected by initial pH. Other investigators have also found that initial pH exerts little impact on ammonia degradation while current density and Cl^- concentration appear to be the rate-determining parameters (Li and Liu, 2009; Xiao et al., 2009). Results showing the effects of initial ammonium concentrations and current density are provided in the supplementary information (Figs. S5 and S6).

Fig. 3 shows the temporal variation in Cl^- and active chlorine concentrations during ammonia oxidation. In all cases, the concentration of Cl^- was relatively stable until NH_4^+-N was completely

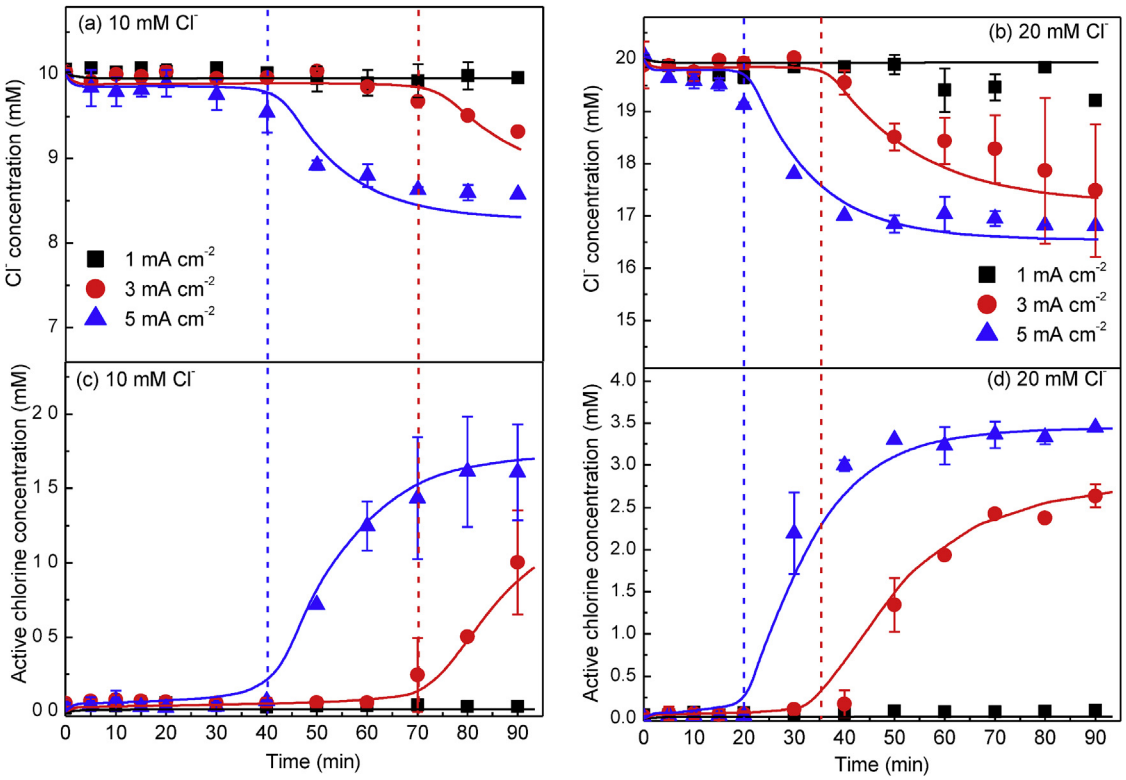

Fig. 3. Temporal variation of chlorine species in the electrochemical system treating wastewater containing 50 mg L^{-1} NH_4^+-N. Chloride with an initial concentration of (a) 10 mM and (b) 20 mM, and active chlorine with an initial Cl^- concentration of (a) 10 mM and (b) 20 mM. Initial pH 6.0. Solid lines represent the results of kinetic modelling. The dotted lines represent the turning point where the Cl^- start to decrease and active chlorine concentration begin to accumulate.

removed. Specifically, obvious decrease in the Cl^- concentration occurred following 70 and 40 min reaction at 3 and 5 mA cm^{-2} at an initial Cl^- of 10 mM (Fig. 3a) while increase in the initial Cl^- concentration to 20 mM resulted in a similar but earlier decrease in Cl^- concentrations (Fig. 3b). In comparison, when the current density was fixed at 1 mA cm^{-2}, no significant change in chloride concentrations was observed with this result likely associated with the residual of ammonia in the solutions over the course of the experiments (Fig. 2).

Active chlorine was also monitored as it plays a crucial role in ammonia removal through the aforementioned reactions (Eqs (2)–(4)). Initially, a low concentration of active chlorine was detected due to its rapid consumption in the indirect ammonia oxidation process while it increased to a relatively high value following the complete degradation of ammonia (Fig. 3c and d). With the use of 10 mM Cl^-, active chlorine began to accumulate from 40 min to 70 min at current densities of 5to3 mA cm^{-2}, respectively. For a higher initial Cl^- concentration of 20 mM, the concentration of active chlorine increased earlier (Fig. 3d). It should be noted that the steady-state concentrations of resultant active chlorine were quite comparable to the control experiments (Fig. 1). In contrast, the active chlorine concentrations were low throughout the whole electrolysis process at 1 mA cm^{-2}.

It is expected that the electrochemical ammonia oxidation process commences with the anodic oxidation of Cl^- to active chlorine which subsequently reacts with ammonia resulting in the production of nitrogen gas (Eqs (2)–(4)). Meanwhile, active chlorine is reduced to Cl^-. The dashed lines in Fig. 3 represent the time up until which the Cl^- concentration does not change significantly and active chlorine does not accumulate as (prior to these critical times) it is reacting with ammonia that is still present As such, Cl^- can be regarded as a "catalyst" for electrochemical ammonia degradation up to these times. However, once the concentration of ammonia has decreased to zero, the Cl^- concentration begins to decrease with active chlorine thereafter accumulating in a manner similar to that shown in Fig. 1.

3.3. By-products generation

The generation of hazardous by-products such as chlorate and perchlorate is one main drawback of EAOPs applied to water/wastewater containing chloride. In our system, chlorate was the only chloro-species detected in all conditions with the concentrations of perchlorate well below the detection limit.

The formation of chlorate during the electrolysis of the solution without ammonia is shown in Fig. 4a and b. Relatively low concentrations of chlorate were generated at the lowest current density applied (1 mA cm^{-2}). Not surprisingly, chlorate concentration increased on increasing the applied current density to 5 mA cm^{-2} with 112 and 193 μM chlorate produced after 90 min electrolysis of solutions containing 10 mM and 20 mM Cl^-. Nevertheless, the final chlorate concentrations in this electrochemical cell were less than 1% of the initial Cl^- concentration, which is one order of magnitude lower than those observed in other similar electrochemical ammonia removal systems (Jung et al., 2010; Lin et al., 2016), suggesting that by-products generation was suppressed in our cell.

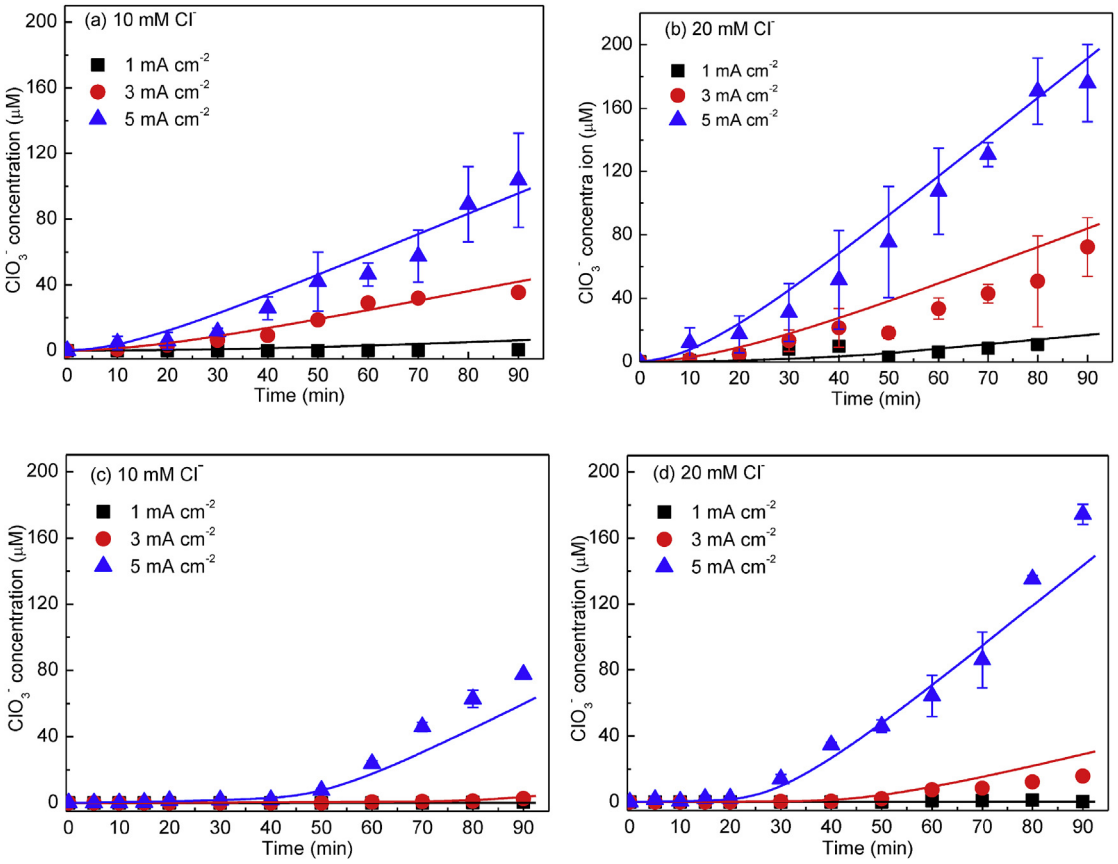

Fig. 4. Formation of chlorate at different current densities in solutions containing no ammonia and (a) 10 mM and (b) 20 mM initial chloride, and solutions containing 50 mg L^{-1} ammonia and (c) 10 mM and (d) 20 mM initial chloride. Initial pH 6.0. Solid lines represent the results of kinetic modelling.

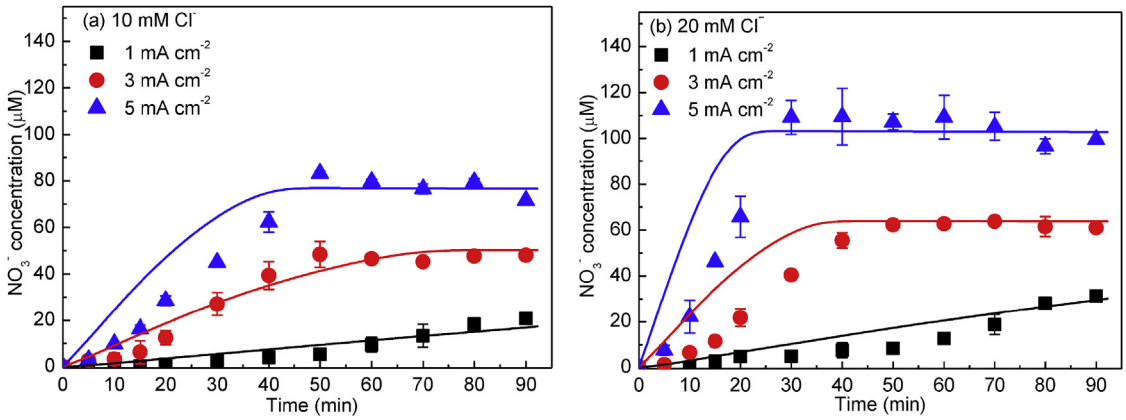

Fig. 5. Formation of nitrate at different current densities with initial Cl^- concentration of (a) 10 mM, and (b) 20 mM. Initial pH 6.0. Solid lines represent the results of kinetic modelling.

When ammonia was present in the electrolyte, as shown in Fig. 4c and d, the formation of chlorate was initially inhibited but increased rapidly once ammonia had been completely removed (as a result of oxidation by electro-generated chlorine). With an initial Cl^- concentration of 10 mM, the chlorate concentration reached 0.5, 1.2 and 1.9 μM at the time point when most ammonia was removed at current densities of 1, 3 and 5 mA cm^{-2}, respectively. For a higher initial Cl^- concentration (Fig. 4d), the chlorate generation was relatively faster, with 1.2, 2.0 and 2.4 μM formed at the end of the ammonia removal period for current densities, respectively, of 1, 3 and 5 mA cm^{-2}. These values are lower than the guideline (8.4 μM) suggested by WHO (WHO, 2011) though once ammonia was exhausted, the chlorate production exhibited a similar trend to the ammonia-free cases (Fig. 4a and b) with the chlorate concentrations increasing to more than 100 μM following 90 min of reaction.

During the sequential oxidation of ammonia with *in situ* generated free chlorine, most of the ammonia would be expected to convert to N_2 (Reactions 7–10 in Table 1) though a portion could transform into other nitrogenous by-products such as nitrite and

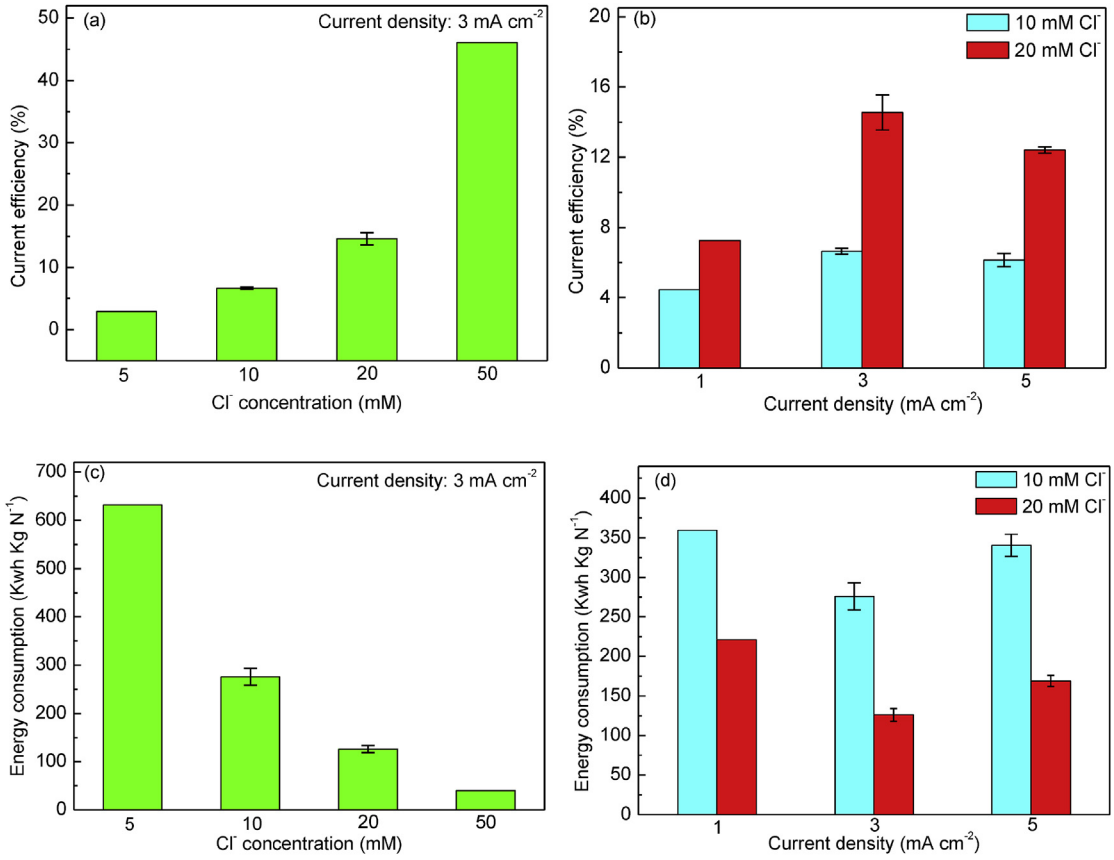

Fig. 6. Current efficiency (a) as a function of Cl^- concentration at a constant current density of 3 mA cm^{-2} and (b) as a function of current density for solutions containing 10 mM and 20 mM Cl^-. Energy consumption (c) as a function of Cl^- concentration at a constant current density of 3 mA cm^{-2} and (d) as a function of current density. Initial pH 6.0 in all scenarios.

nitrate via reactions such as that shown in Eq (7):

$$NH_4^+ + 4HOCl \rightarrow NO_3^- + H_2O + 6H^+ + 4Cl^- \quad (7)$$

In all experiments described here, the concentration of nitrite was below the detection limit while a small quantity of nitrate was observed. Typical profiles of nitrate formation are shown in Fig. 5 with the production of nitrate commencing at the beginning of each experiment and the concentration increasing continuously until a plateau was reached at approximately the time at which ammonia was totally removed. The generation rate of nitrate increased with increase in current density and initial Cl^- concentration with the nitrate concentration reaching more than 100 μM when 5 mA cm^{-2} current density and 20 mM Cl^- were used. Nevertheless, this value is far below drinking water guideline values (806 μM) (WHO, 2011). Due to very limited information on steady-state concentration of nitrite, only an overall reaction (Reaction 12 in Table 1) has been introduced to the kinetic model with a reasonable description of formation of nitrate achieved from the kinetic modelling of our experimental data (Fig. 5). Possible pH dependence of the rate of this reaction could account for the small differences observed between model and experimental values. Chloramine is, potentially, another nitrogen by-product that could be formed during the active chlorine mediated ammonia oxidation process. In our experiments, however, minimal concentrations of chloramine (<10 μM) were detected after 90 min electrolysis with this accounting for less than 0.5% of the initial NH_4^+-N concentration (data not shown).

3.4. Current efficiency and energy consumption

As mentioned earlier, current efficiency and energy consumption are two key parameters used to evaluate the performance of electrochemical processes. As illustrated in Fig. 6a, at a current density of 3 mA cm^{-2}, the current efficiency (*CE*) was 2.9% for a 5 mM Cl^- solution but increased sharply to 6.7%, 14.6%, and 46.1% if higher Cl^-concentrations of 10, 20 and 50 mM were employed. Results presented in Fig. 6b indicate that the current efficiency first increased with increase in current density and then decreased, with the maximum value achieved at 3 mA cm^{-2}. In contrast, energy consumption exhibits a negative relationship with Cl^- concentration. The electrochemical cell operated with initial Cl^- concentration of 50 mM and current density of 3 mA cm^{-2} consumed the lowest energy (39.9 kWh kg N^{-1}) of the various operating conditions examined with this value one order of magnitude lower than that reported in previous work (Yang et al., 2016) (Fig. 6c and d).

4. Discussion

Although the electrochemical ammonia oxidation process has now been described by a number of investigators, understanding of the detailed mechanism of chlorine evolution and ammonia removal remains relatively preliminary. To assist our understanding, we here-in develop a mechanistically-based kinetic model to describe the anodic chlorine evolution and the resultant indirect ammonia oxidation processes. The core components of the model include (i) active chlorine evolution during the electrolysis of NaCl solution (in the absence of ammonia) and (ii) indirect ammonia oxidation by *in situ* generated active chlorine (Table 1).

4.1. Active chlorine evolution

The *in situ* electro-generated free chlorine is recognized to be the principal agent responsible for the oxidation of ammonia. Fig. 1 shows the electrolytic generation of chlorine in the absence of ammonia with the observed behaviour following the classical Volmer-Heyrovsky (V-H) mechanism (Hansen et al., 2010; Trasatti, 1987). According to this mechanism, chloride ion is first adsorbed on the metal-oxide electrode and is transformed into the chloride radical and, in the process, releases an electron (Reaction 1 in Table 1):

$$MO_x + Cl^- \xrightarrow{k_1} MO_x(Cl^\bullet) + e^- \quad (8)$$

In the following Heyrovsky step, the generated $Cl^\bullet$ combines with the Cl^- near the electrodes to produce chlorine (Reaction 2 in Table 1):

$$MO_x(Cl^\bullet) + Cl^- \xrightarrow{k_2} MO_x + Cl_2 + e^- \quad (9)$$

Alternatively, two $Cl^\bullet$ radicals can combine and generate chlorine through the Volmer-Tafel reaction (Reaction 3 in Table 1):

$$MO_x(Cl^\bullet) + MO_x(Cl^\bullet) \xrightarrow{k_3} 2MO_x + Cl_2 \quad (10)$$

Subsequently, the hydrolysis of Cl_2 occurs (Reaction 4 in Table 1):

$$Cl_2 + H_2O \xrightarrow{k_4} HOCl + H^+ + Cl^- \quad (11)$$

The hypochlorous acid generated at the anode can then be reduced to chloride ion at the cathode surface (Reaction 5 in Table 1):

$$HOCl + 2e^- \xrightarrow{k_5} Cl^- + OH^- \quad (12)$$

The main side reactions involve the further anodic oxidation of $HOCl/OCl^-$ to chlorate (Reaction 6 in Table 1) (Yang et al., 2016):

$$MO_x(2H_2O) + HOCl \xrightarrow{k_6} MO_x + ClO_3^- + 5H^+ + 4e^- \quad (13)$$

Here, reaction 1 and reaction 5 in Table 1 are the two key reactions that determine formation and decay of active chlorine while reaction 6 has an insignificant effect as the transformation of active chlorine to chlorate is negligible. Indeed, the active chlorine concentration was controlled by the ratio of reactions 1 and 5. By maintaining the ratio of the rate constants for reactions 1 and 5 constant at each current density, we can obtain the values of these rate constants on the basis of best fit to the experimental data for formation of active chlorine and decay of Cl^- (Fig. 1).

As illustrated in Table 1, the rate constants of reactions 1 and 5 (k_1 and k_5) showed a strong dependency on current density. For instance, the rate constant of $Cl^\bullet$ formation (k_1) increased from $0.2 \times 10^{-4}\ s^{-1}$ to $2.3 \times 10^{-4}\ s^{-1}$ as the applied current density increased from 1 mA cm^{-2} to 5 mA cm^{-2}. Meanwhile, the cathodic chlorine reduction reaction exhibited a rate constant ranging from $1.8 \times 10^{-4}\ s^{-1}$ to $11 \times 10^{-4}\ s^{-1}$ with its occurrence leading to the achievement of steady-state concentrations of active chlorine (Fig. 1). Fig. S7 shows that the values of these rate constants correlate linearly with the current densities ($R^2 > 0.98$). The rate constant for reaction 6 was obtained by fitting the experimental data for chlorate generation (Fig. 4a and b).

It should be noted that the rate and extent of generation of active chlorine is largely determined by the nature of the anode materials used. In previous work, linear sweep voltammetry was used to determine the active chlorine evolution potentials of the three most widely used EAOP electrodes (i.e., BDD, Ti/IrO_2-RuO_2 and Ti/IrO_2-Ta_2O_5). Of these electrodes, Ti/IrO_2-RuO_2 exhibited a lower chlorine evolution potential (1.10 V vs. SCE) than Ti/IrO_2-Ta_2O_5 (1.11 V vs. SCE) and BDD anodes (1.98 V vs. SCE) with this comparison indicating that active chlorine production (reaction

1–4) should be more facile at a Ti/IrO_2-RuO_2 anode than at a BDD anode on application of the same voltage (Zhou et al., 2011). Moreover, mixed metal oxides such as IrO_2-RuO_2 have been found to increase the activity, selectivity and stability of the anode with these materials providing active sites for radical ($Cl^{\bullet}$) formation and the redox transitions of RuO_x (V/IV) and IrO_x (IV/VI) serving as electron sinks (Arikawa et al., 1998; Ferro and De Battisti, 2002). In our EAOP system, the rate constant for $Cl^{\bullet}$ formation (k_1) on the Ti/IrO_2-RuO_2 anode used was more than one order larger than that obtained in previous similar work using a multilayer heterojunction SbSn/CoTi/Ir anode (Yang et al., 2016).

Chlorate appeared to be the only stable chloride-related by-product generated during the electrolysis process with perchlorate concentrations below detection limit. As illustrated in Table 1, the chlorate formation rate constant (k_6) is two orders of magnitude lower than k_1 with this result in line with previous findings that the IrO_2-RuO_2 anode is conducive to catalysing the generation of active chlorine but, satisfyingly, does little to facilitate the conversion of chlorine to by-products such as chlorate and perchlorate (Bagastyo et al., 2011; Zöllig et al., 2015c).

4.2. Chlorine-mediated ammonia oxidation

As the identity and rate constants for the key reactions of the traditional breakpoint chlorination process have been reasonably well established, we combined the established ammonia reaction set (reaction 7–12 in Table 1) with the reactions describing the electrochemical active chlorine evolution (reaction 1–6 in Table 1) in order to fully elucidate the mechanism and kinetics of the electrochemically assisted ammonia oxidation processes. It should be noted that reaction 5 in Table 1 actually plays a minor role in the kinetic model of ammonia oxidation since the *in-situ* generated active chlorine will be immediately consumed near the anode surface when ammonia is present in solution thereby rendering the cathodic chlorine reduction reaction (reaction 5 in Table 1) unlikely to occur.

As can be seen from Fig. 2, the reaction set we present in Table 1 is able to satisfactorily describe the ammonia degradation data over a range of conditions including different current densities and initial Cl^- concentrations. The model also provides an excellent description of the time varying concentrations of Cl^- (Fig. 3a and b) and active chlorine (Fig. 3c and d) as well as by-products chlorate (Fig. 4c and d) and nitrate (Fig. 5a and b). As illustrated Table 1, the *in situ* generated active chlorine could react with ammonia and form monochloramine and then dichloramine with rate constants for these reactions of $3.1 \times 10^6\ M^{-1}\ s^{-1}$ and $1.5 \times 10^2\ M^{-1}\ s^{-1}$ respectively. Dichloramine, on the one hand, could decompose into NOH, which could combine with monochloramine and dichloramine resulting in formation of harmless nitrogen gas with rate constants of $8.3 \times 10^3\ M^{-1}\ s^{-1}$ and $2.8 \times 10^4\ M^{-1}\ s^{-1}$, respectively. The oxidation of ammonium ions via reaction with $Cl^{\bullet}$ is unimportant in our system because of (i) the much higher concentration of Cl^- than NH_4^+ and (ii) $Cl^{\bullet}$ is generated at the anode to which positively charged NH_4^+ ions cannot approach. For these reasons, the transformations of $Cl^{\bullet}$ into active chlorine (reaction 2 and 3 in Table 1) are the dominant reactions while the reactions between $Cl^{\bullet}$ and NH_4^+ are of minor importance.

Sensitivity analysis was undertaken in order to determine the importance of each of the various reactions (Table 1) in the kinetic model towards ammonia degradation during the electrolysis process. As shown in Fig. S7, the oxidation of the chloride ion to the chloride radical (reaction 1) is the only dominant reaction in the chlorine evolution reaction set, while the transformation of NH_4^+ into NH_2Cl (reaction 7) and its subsequent decomposition into harmless N_2 (reaction 10) play relatively significant roles in relation to the ultimate degradation of ammonia compounds.

Ammonia nitrogen removal from real wastewaters (*i.e.,* domestic sources, landfills, tanneries and urine) using electrochemical advanced oxidation processes (EAOP) has been examined previously by a number of investigators. For example, greater than 95% reductions in COD and NH_4^+-N were observed within 6h on treating decentralized domestic wastewater (influent NH_4^+-N concentration of 30–40 mg L^{-1}, COD concentration of 400 mg L^{-1} and Cl^- concentration of 10–50 mM) using an EAOP (Cho et al., 2014; Yang et al., 2016). The effluent from this EAOP was of high quality and was considered suitable for nonpotable applications such as toilet flushing and it was proposed that the hydrogen gas generated at the cathode could be used as a back-up energy source for the EAOP system. EAOP have also been proposed as an effective alternative method for indirect ammonium oxidation from landfill leachate as the presence of high chloride concentrations are considered likely to facilitate this process (Anglada et al., 2009, 2011; Cabeza et al., 2007; Pérez et al., 2012b). Undesired chloride related by-products (*i.e.,* chloramine, chlorate and perchlorate) were generated on

Table 1
Proposed model and rate constants for the electrochemical ammonia oxidation process.

No.	Reaction	Rate constant	References
Active chlorine evolution			
1	$MO_x + Cl^- \rightarrow MO_x(Cl^{\bullet}) + e^-$	1 mA cm^{-2}: $0.2 \times 10^{-4}\ s^{-1}$ 3 mA cm^{-2}: $1.3 \times 10^{-4}\ s^{-1}$ 5 mA cm^{-2}: $2.3 \times 10^{-4}\ s^{-1}$	This study
2	$MO_x(Cl^{\bullet}) + Cl^- \rightarrow MO_x + Cl_2 + e^-$	$>1.0 \times 10^5\ M^{-1}\ s^{-1}$	This study
3	$MO_x(Cl^{\bullet}) + MO_x(Cl^{\bullet}) \rightarrow 2MO_x + Cl_2$	$1.0 \times 10^8\ M^{-1}\ s^{-1}$	(Wu et al., 1980)
4	$Cl_2 + H_2O \rightarrow HOCl + H^+ + Cl^-$	$0.52\ M^{-1}\ s^{-1}$	(Wang and Margerum, 1994)
5	$HOCl + 2e^- \rightarrow Cl^- + OH^-$	1 mA cm^{-2}: $1.8 \times 10^{-4}\ s^{-1}$ 3 mA cm^{-2}: $7.5 \times 10^{-4}\ s^{-1}$ 5 mA cm^{-2}: $11 \times 10^{-4}\ s^{-1}$	This study
6	$MO_x(2H_2O) + HOCl \rightarrow MO_x + ClO_3^- + 5H^+ + 4e^-$	1 mA cm^{-2}: $2.4 \times 10^{-6}\ s^{-1}$ 3 mA cm^{-2}: $6.7 \times 10^{-6}\ s^{-1}$ 5 mA cm^{-2}: $12 \times 10^{-6}\ s^{-1}$	This study
Active chlorine-mediated ammonia oxidation			
7	$NH_4^+ + HOCl \rightarrow NH_2Cl + H^+ + H_2O$	$3.1 \times 10^6\ M^{-1}\ s^{-1}$	(Qiang and Adams, 2004)
8	$NH_2Cl + HOCl \rightarrow NHCl_2 + H_2O$	$1.5 \times 10^2\ M^{-1}\ s^{-1}$	(Mergerum et al., 1978)
9	$NHCl_2 + H_2O \rightarrow NOH + 2H^+ + 2Cl^{\bullet}$	$1.7 \times 10^2\ M^{-1}\ s^{-1}$	(Zhang et al., 2015)
10	$NH_2Cl + NOH \rightarrow N_2 + H^+ + Cl^- + H_2O$	$8.3 \times 10^3\ M^{-1}\ s^{-1}$	(Zhang et al., 2015)
11	$NHCl_2 + NOH \rightarrow N_2 + 2H^+ + 2Cl^- + H_2O$	$2.8 \times 10^4\ M^{-1}\ s^{-1}$	(Zhang et al., 2015)
12	$NH_4^+ + 4HOCl \rightarrow NO_3^- + 3H_2O + 6H^+ + 4Cl^-$	$0.1–0.7\ M^{-1}\ s^{-1}$	This study

electrolysis of real landfill leachate but, by adjusting the parameters such as applied current density and influent chloride concentration, the generation of chloramine and perchlorate could be effectively eliminated (Pérez et al., 2012b).

While the energy consumption is substantially higher than that of conventional biological processes, EAOP provides a feasible approach for treating ammonia-containing wastewaters with lower area requirement, easier maintenance and remarkably reproducible behavior. In addition, no secondary waste biomass is generated. Consideration should be given to use of EAOP as a final polishing step or as an alternative technology to biological nitrification with this latter option particularly attractive for chloride-containing wastewaters. Future work will be undertaken to achieve better ammonium removal performance, to further reduce the energy demand and to minimize toxic by-products formation.

4.3. Implications of the model

The mechanistically-based kinetic model developed here provides an effective method to both interpret the experimental data and determine optimal conditions for ammonia oxidation with minimal generation of undesirable by-products. The ammonia degradation times predicted to be required using the kinetic model for complete ammonia removal for a range of initial Cl^- and ammonia concentrations are shown in Fig. 7 for current densities of 3 mA cm^{-2} (Fig. 7a) and 5 mA cm^{-2} (Fig. 7b). Utilizing Fig. 7, we can readily determine the appropriate operating time for ammonia removal for particular influent water compositions. If the operating time is shorter than that deduced using the model, ammonia is unlikely to be completely oxidized. However, if an operating time longer than that predicated is used, all of the incoming ammonia will be degraded with residual active chlorine transferred to and

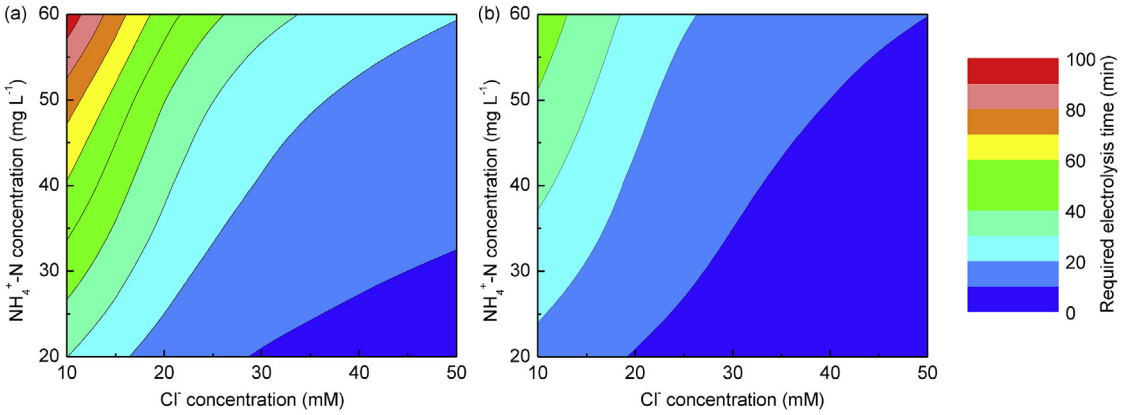

Fig. 7. Prediction (deduced by use of the kinetic model developed in this work) of the electrolysis time required for complete ammonia oxidation as a function of source water chloride and ammonia concentrations at constant current densities of (a) 3 mA cm^{-2} and (b) 5 mA cm^{-2}. An initial pH of 6.0 was assumed in all scenarios.

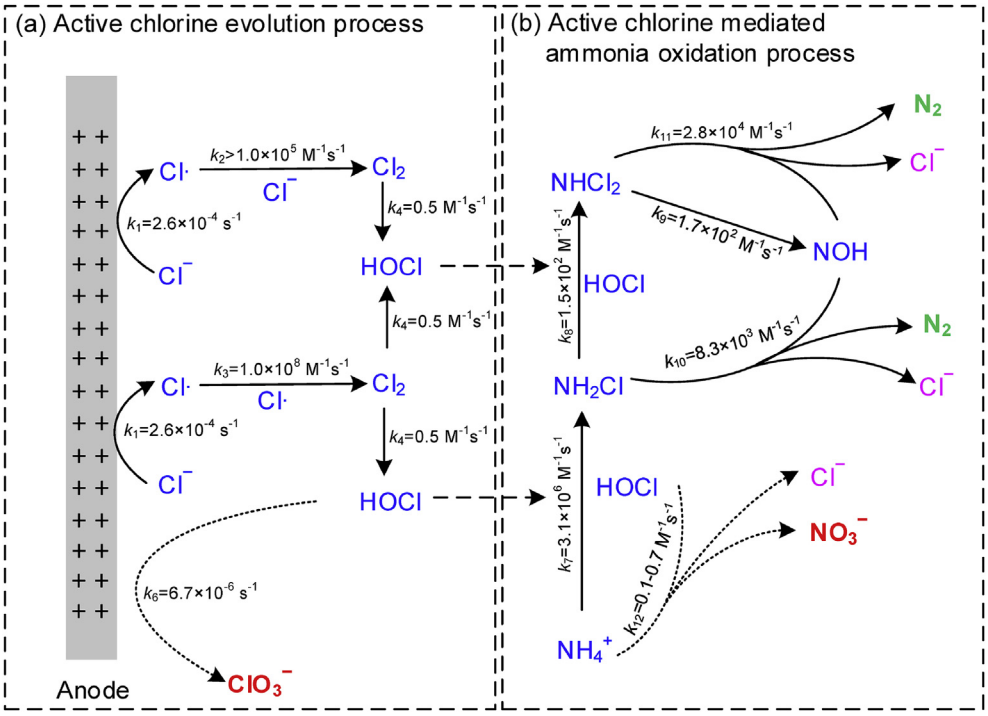

Fig. 8. Proposed reaction pathways and reaction rate constants for ammonia degradation by electrochemically generated active chlorine. The schematic shows both (a) active chlorine evolution at the anode, and (b) active chlorine mediated ammonia oxidation. Final products are indicated in bold characters.

consumed at the cathode (Eq (5) in Table 1). This not only results in a sharp decrease in current efficiency and increase in energy consumption, but also results in the formation of excessive by-products (Fig. 4c and d).

Based on the experimental and modelling results, a reaction mechanism for the electrochemical active chlorine-mediated ammonia oxidation process is proposed and shown in Fig. 8. The initial activation of Cl^- to $Cl^\bullet$ results in the formation of active chlorine. The mono/dichloramine generated from the reaction between active chlorine and ammonia undergoes rapid cleavage with the aid of a local excess of active chlorine with eventual transformation to nitrogen gas. Cl^- can be regenerated during the oxidation of ammonia with the reformation of Cl^- facilitating the anodic production of active chlorine thereby extending the lifetime of Cl^- and allowing Cl^- to be employed in catalytic quantities. Only trace amounts of chlorine and nitrogen by-products are produced.

In break-point oxidation of ammonia, when the active chlorine dose to ammonia-nitrogen molar ratio (Cl/N) is lower than 1, active chlorine reacts with ammonia and converts it into chloramine with the concentration of total nitrogen remaining constant while in the transition region ($1 < Cl/N < 1.6$), decay of ammonia and chloramine starts to occur. At $Cl/N > 1.6$, complete removal of ammonia nitrogen to nitrogen gas is achieved. In contrast, during the electrochemical ammonia oxidation in the presence of Cl^-, removal of ammonia nitrogen is initiated at the very beginning of the electrolysis process. This is attributed to the high localized concentration of *in situ* electro-generated active chlorine, with the molar ratio between ammonia nitrogen likely to be higher than 1.6 in the reaction zone close to the anode surface, resulting in the rapid transformation of ammonia to chloramine followed by complete decomposition into nitrogen gas prior to diffusion into bulk solution. It is therefore apparent that the electrochemical oxidation method has advantages over classical break-point chlorination treatment in view of the more efficient use of *in situ* generated active chlorine, the suppression of generation/accumulation of nitrogen by-products.

5. Conclusion

We have demonstrated in this study that the active chlorine-mediated electrochemical oxidation of ammonia can be an effective technology for ammonia removal. The *in situ* generated active chlorine can be used to efficiently convert ammonia into harmless nitrogen gas with concentrations of by-products (i.e., chlorate, nitrate and chloramine) well below WHO guidelines. A mechanistically-based kinetic model has been developed that successfully describes the key underlying reactions occurring in the electrochemical ammonia oxidation system, including active chlorine evolution, ammonia decomposition, and by-product formation. This model can be used to determine operating conditions (current densities, electrolysis times) appropriate to particular feed water compositions (of chloride and ammonia content) that enable complete ammonia removal at optimal current efficiency and minimal by-product formation. These findings contribute to our fundamental understanding of the electrochemical oxidation of ammonia and provide guidance with regard to effective implementation and optimization of this process.

Acknowledgement

We gratefully acknowledge funding support from the Australian Research Council through ARC Linkage Grant LP150100854. Support for Dr. Jinxing Ma through a UNSW Vice Chancellor's Postdoctoral Fellowship is gratefully acknowledged. The authors also thank Dr. Guowei Xing for his support in undertaking sensitivity analysis using Kintecus.

Appendix A. Supplementary data

Supplementary data related to this article can be found at https://doi.org/10.1016/j.watres.2018.08.025.

References

Anglada, A., Urtiaga, A., Ortiz, I., 2009. Pilot scale performance of the electrooxidation of landfill leachate at boron-doped diamond anodes. Environ. Sci. Technol. 43 (6), 2035–2040.

Anglada, A., Urtiaga, A., Ortiz, I., Mantzavinos, D., Diamadopoulos, E., 2011. Boron-doped diamond anodic treatment of landfill leachate: evaluation of operating variables and formation of oxidation by-products. Water Res. 45 (2), 828–838.

APHA, 2012. Standard Methods for the Examination of Water and Wastewater, twenty-second ed. American Public Health Association (APHA), Washington, DC, USA.

Arikawa, T., Takasu, Y., Murakami, Y., Asakura, K., Iwasawa, Y., 1998. Characterization of the structure of RuO_2–IrO_2/Ti electrodes by EXAFS. J. Phys. Chem. B 102 (19), 3736–3741.

Bagastyo, A.Y., Radjenovic, J., Mu, Y., Rozendal, R.A., Batstone, D.J., Rabaey, K., 2011. Electrochemical oxidation of reverse osmosis concentrate on mixed metal oxide (MMO) titanium coated electrodes. Water Res. 45 (16), 4951–4959.

Bonmatı, A., Flotats, X., 2003. Air stripping of ammonia from pig slurry: characterisation and feasibility as a pre-or post-treatment to mesophilic anaerobic digestion. Waste Manag. 23 (3), 261–272.

Buffle, M.-O., Galli, S., Von Gunten, U., 2004. Enhanced bromate control during ozonation: the chlorine-ammonia process. Environ. Sci. Technol. 38 (19), 5187–5195.

Cabeza, A., Urtiaga, A., Rivero, M.J., Ortiz, I., 2007. Ammonium removal from landfill leachate by anodic oxidation. J. Hazard Mater. 144 (3), 715–719.

Cho, K., Qu, Y., Kwon, D., Zhang, H., Cid, C.A., Aryanfar, A., Hoffmann, M.R., 2014. Effects of anodic potential and chloride ion on overall reactivity in electrochemical reactors designed for solar-powered wastewater treatment. Environ. Sci. Technol. 48 (4), 2377–2384.

Ferro, S., De Battisti, A., 2002. Electrocatalysis and chlorine evolution reaction at ruthenium dioxide deposited on conductive diamond. J. Phys. Chem. B 106 (9), 2249–2254.

Hansen, H.A., Man, I.C., Studt, F., Abild-Pedersen, F., Bligaard, T., Rossmeisl, J., 2010. Electrochemical chlorine evolution at rutile oxide (110) surfaces. Phys. Chem. Chem. Phys. 12 (1), 283–290.

Huang, L., Li, L., Dong, W., Liu, Y., Hou, H., 2008. Removal of ammonia by OH radical in aqueous phase. Environ. Sci. Technol. 42 (21), 8070–8075.

Ji, Y., Bai, J., Li, J., Luo, T., Qiao, L., Zeng, Q., Zhou, B., 2017. Highly selective transformation of ammonia nitrogen to N2 based on a novel solar-driven photo-electrocatalytic-chlorine radical reactions system. Water Res. 125, 512–519.

Johnson, K.A., Simpson, Z.B., Blom, T., 2009. Global Kinetic Explorer: a new computer program for dynamic simulation and fitting of kinetic data. Anal. Biochem. 387, 20–29.

Jorgensen, T., Weatherley, L., 2003. Ammonia removal from wastewater by ion exchange in the presence of organic contaminants. Water Res. 37 (8), 1723–1728.

Jung, Y.J., Baek, K.W., Oh, B.S., Kang, J.W., 2010. An investigation of the formation of chlorate and perchlorate during electrolysis using Pt/Ti electrodes: the effects of pH and reactive oxygen species and the results of kinetic studies. Water Res. 44 (18), 5345–5355.

Kalyuzhnyi, S., Gladchenko, M., Mulder, A., Versprille, B., 2006. DEAMOX—new biological nitrogen removal process based on anaerobic ammonia oxidation coupled to sulphide-driven conversion of nitrate into nitrite. Water Res. 40 (19), 3637–3645.

Kapałka, A., Joss, L., Anglada, Á., Comninellis, C., Udert, K.M., 2010. Direct and mediated electrochemical oxidation of ammonia on boron-doped diamond electrode. Electrochem. Commun. 12 (12), 1714–1717.

Kim, K.W., Kim, Y.J., Kim, I.T., Park, G.I., Lee, E.H., 2006. Electrochemical conversion characteristics of ammonia to nitrogen. Water Res. 40 (7), 1431–1441.

Li, L., Liu, Y., 2009. Ammonia removal in electrochemical oxidation: mechanism and pseudo-kinetics. J. Hazard Mater. 161 (2–3), 1010–1016.

Li, X., Zhao, Q., Hao, X., 1999. Ammonium removal from landfill leachate by chemical precipitation. Waste Manag. 19 (6), 409–415.

Lin, Z., Yao, W., Wang, Y., Yu, G., Deng, S., Huang, J., Wang, B., 2016. Perchlorate formation during the electro-peroxone treatment of chloride-containing water: effects of operational parameters and control strategies. Water Res. 88, 691–702.

Ma, J., He, C., He, D., Zhang, C., Waite, T.D., 2018. Analysis of capacitive and electrodialytic contributions to water desalination by flow-electrode CDI. Water Res. https://doi.org/10.1016/j.watres.2018.07.049.

Mergerum, D.W., Gray, J.R.,E.T., Huffman, R.P.H., 1978. Chlorination and the formation of N-chloro compounds in water treatment. In: Brinckman, F.E., Bellama, J.M. (Eds.), Organometals and Organometaloids: Occurrence and Fate in the Environment. ACS Books, Washington, DC, pp. 278–291.

Obaid-ur-Rehman, S., Beg, S., 1990. Ammonia removal by air stripping-from origin

to present state of technology. J. Environ. Sci. Heal. A 25 (4), 343–365.
Pérez, G., Ibáñez, R., Urtiaga, A.M., Ortiz, I., 2012a. Kinetic study of the simultaneous electrochemical removal of aqueous nitrogen compounds using BDD electrodes. Chem. Eng. J. 197, 475–482.
Pérez, G., Saiz, J., Ibañez, R., Urtiaga, A.M., Ortiz, I., 2012b. Assessment of the formation of inorganic oxidation by-products during the electrocatalytic treatment of ammonium from landfill leachates. Water Res. 46 (8), 2579–2590.
Pham, A.N., Waite, T.D., 2008. Oxygenation of Fe (II) in natural waters revisited: kinetic modeling approaches, rate constant estimation and the importance of various reaction pathways. Geochem. Cosmochim. Acta 72 (15), 3616–3630.
Pressley, T.A., Bishop, D.F., Roan, S.G., 1972. Ammonia-nitrogen removal by breakpoint chlorination. Environ. Sci. Technol. 6 (7), 622–628.
Qiang, Z., Adams, C.D., 2004. Determination of monochloramine formation rate constants with stopped-flow spectrophotometry. Environ. Sci. Technol. 38 (5), 1435–1444.
Qiu, S., He, D., Ma, J., Liu, T., Waite, T.D., 2015. Kinetic modeling of the electro-Fenton process: quantification of reactive oxygen species generation. Electrochim. Acta 176, 51–58.
Ruiz, G., Jeison, D., Chamy, R., 2003. Nitrification with high nitrite accumulation for the treatment of wastewater with high ammonia concentration. Water Res. 37 (6), 1371–1377.
Tarpeh, W.A., Barazesh, J.M., Cath, T.Y., Nelson, K.L., 2018. Electrochemical stripping to recover nitrogen from source-separated urine. Environ. Sci. Technol. 52 (3), 1453–1460.
Trasatti, S., 1987. Progress in the understanding of the mechanism of chlorine evolution at oxide electrodes. Electrochim. Acta 32 (3), 369–382.
Vajda, S., Valko, P., Turanyi, T., 1985. Principal component analysis of kinetic models. Int. J. Chem. Kinet. 17 (1), 55–81.
Vanlangendonck, Y., Corbisier, D., Van Lierde, A., 2005. Influence of operating conditions on the ammonia electro-oxidation rate in wastewaters from power plants (ELONITA technique). Water Res. 39 (13), 3028–3034.
Vlyssides, A.G., Israilides, C.J., 1997. Detoxification of tannery waste liquors with an electrolysis system. Environ. Pollut. 97 (1–2), 147–152.
Wang, T.X., Margerum, D.W., 1994. Kinetics of reversible chlorine hydrolysis-temperature-dependence and general acid base-assisted mechanisms. Inorg. Chem. 33 (6), 1050–1055.
Wang, Y., Liu, S., Xu, Z., Han, T., Chuan, S., Zhu, T., 2006. Ammonia removal from leachate solution using natural Chinese clinoptilolite. J. Hazard Mater. 136 (3), 735–740.
WHO, 2011. Guidelines for drinking-water quality. WHO Chron. 38, 104–108.
Wu, D., Wong, D., Di Bartolo, B., 1980. Evolution of Cl2− in aqueous NaCl solutions. J. Photochem. 14 (4), 303–310.
Xiao, S., Qu, J., Zhao, X., Liu, H., Wan, D., 2009. Electrochemical process combined with UV light irradiation for synergistic degradation of ammonia in chloride-containing solutions. Water Res. 43 (5), 1432–1440.
Xing, G., Pham, A.N., Miller, C.J., Waite, T.D., 2018. pH-dependence of production of oxidants (Cu(III) and/or HO •) by copper-catalyzed decomposition of hydrogen peroxide under conditions typical of natural saline waters. Geochem. Cosmochim. Acta 232, 30–47.
Yang, Y., Shin, J., Jasper, J.T., Hoffmann, M.R., 2016. Multilayer heterojunction anodes for saline wastewater treatment: design strategies and reactive species generation mechanisms. Environ. Sci. Technol. 50 (16), 8780–8787.
Ye, Z., Zhang, H., Zhang, X., Zhou, D., 2016. Treatment of landfill leachate using electrochemically assisted UV/chlorine process: effect of operating conditions, molecular weight distribution and fluorescence EEM-PARAFAC analysis. Chem. Eng. J. 286, 508–516.
Zhang, C., He, D., Ma, J., Tang, W., Waite, T.D., 2018a. Faradaic reactions in capacitive deionization (CDI) - problems and possibilities: a review. Water Res. 128, 314–330.
Zhang, C., Ma, J., He, D., Waite, T.D., 2017. Capacitive membrane stripping for ammonia recovery (CapAmm) from dilute wastewaters. Environ. Sci. Technol. Lett. 5 (1), 43–49.
Zhang, J., Hanigan, D., Shen, R., Andrews, S., Herckes, P., Westerhoff, P., 2015. Modeling NDMA formation kinetics during chloramination of model compounds and surface waters impacted by wastewater discharges. In: Recent Advances in Disinfection By-products, ACS Symposium Series, vol. 1190. American Chemical Society, Washington, DC, pp. 79–95.
Zhang, Y., Li, J., Bai, J., Shen, Z., Li, L., Xia, L., Chen, S., Zhou, B., 2018b. Exhaustive conversion of inorganic nitrogen to nitrogen gas based on a photoelectrochlorine cycle reaction and a highly selective nitrogen gas generation cathode. Environ. Sci. Technol. https://doi.org/10.1021/acs.est.7b04626.
Zhou, M., Liu, L., Jiao, Y., Wang, Q., Tan, Q., 2011. Treatment of high-salinity reverse osmosis concentrate by electrochemical oxidation on BDD and DSA electrodes. Desalination 277 (1–3), 201–206.
Zöllig, H., Fritzsche, C., Morgenroth, E., Udert, K.M., 2015a. Direct electrochemical oxidation of ammonia on graphite as a treatment option for stored source-separated urine. Water Res. 69, 284–294.
Zöllig, H., Morgenroth, E., Udert, K.M., 2015b. Inhibition of direct electrolytic ammonia oxidation due to a change in local pH. Electrochim. Acta 165, 348–355.
Zöllig, H., Remmele, A., Fritzsche, C., Morgenroth, E., Udert, K.M., 2015c. Formation of chlorination byproducts and their emission pathways in chlorine mediated electro-oxidation of urine on active and nonactive type anodes. Environ. Sci. Technol. 49 (18), 11062–11069.